RESEARCH MEMORANDUM

INVESTIGATION AT MACH NUMBER 1.88 OF HALF OF A CONICAL-SPIKE DIFFUSER MOUNTED AS A SIDE INLET WITH BOUNDARY-LAYER CONTROL

By H. Fred Goelzer and Edgar M. Cortright, Jr.

Lewis Flight Propulsion Laboratory
Cleveland, Ohio

NATIONAL ADVISORY COMMITTEE
FOR AERONAUTICS

WASHINGTON
September 19, 1951

NATIONAL ADVISORY COMMITTEE FOR AERONAUTICS

RESEARCH MEMORANDUM

INVESTIGATION AT MACH NUMBER 1.88 OF HALF OF A CONICAL-SPIKE DIFFUSER MOUNTED AS A SIDE INLET WITH BOUNDARY-LAYER CONTROL

By H. Fred Goelzer and Edgar M. Cortright, Jr.

SUMMARY

An experimental investigation was conducted in a stream of Mach number 1.88 to determine the performance characteristics of a side inlet operating in the presence of initial boundary layer but alined at zero angle of attack and zero yaw with the free stream. The supersonic diffuser consisted of half of a 50°-conical-spike inlet mounted on a flat plate. The subsonic portion of the diffuser was faired into a cylindrical combustion chamber. Boundary-layer removal was accomplished upstream of the inlet by means of a ram-type scoop of variable height. The initial boundary-layer thickness was also varied.

With complete removal of the initial boundary layer upstream of the inlet, a total-pressure recovery of approximately 89 percent was obtained. Allowing all the initial boundary layer to flow into the inlet lowered the inlet total-pressure recovery to approximately 70 percent although the initial defect in total pressure in the boundary layer did not greatly affect the average total pressure upstream of the inlet. Most of the additional losses were determined to occur in the subsonic portion of the diffuser.

The inlet pressure recovery with a simple ram-type scoop having a straight leading edge decreased markedly with decreasing boundary-layer-scoop mass-flow ratio. Several boundary-layer-removal systems were briefly investigated which greatly reduced this sensitivity.

The inlet was subject to large total-pressure losses when operating at zero forward velocity and high throat velocities.

INTRODUCTION

During recent years considerable research has been conducted on air inlets suitable for application to supersonic aircraft or missiles.

This work has been chiefly devoted to axially symmetric spike-type diffusers designed for nose, wing, or pylon installation. Relatively little research is available on the equally important case of the side inlet.

Although the same fundamental types of supersonic diffuser are used, the side-inlet problem is complicated by the need for asymmetrical subsonic diffusers and by the fact that the inlet must operate in the flow field of the body on which it is mounted. With proper removal of the initial boundary layer, proper orientation of the supersonic diffuser with respect to the local stream, and good subsonic diffuser design, the performance of the side inlet should be comparable to its nose inlet counterpart.

One means of alleviating the problems associated with side inlets is to locate the inlets on the underside of the fuselage where the initial boundary layer is generally reduced at a positive angle of attack and the local stream deflections due to angle of attack are minimized. Because total elimination of these effects is not possible, quantitative determination of body-interference effects on diffuser performance is desirable.

This paper considers the case of a conical-spike-type side inlet operating in the presence of an initial boundary layer and alined at zero angle of attack and zero yaw with the local stream of Mach number 1.88. A variable-height ram-type scoop was used to remove the boundary layer upstream of the inlet. In addition several alternative boundary-layer-removal systems were investigated at the NACA Lewis laboratory during this program. The thickness of the initial boundary layer was varied by changing the plate length upstream of the inlet. Both the inlet and the boundary-layer scoop were operated over a range of mass-flow ratios at various values of the boundary-layer-scoop height. In addition, the inlet performance was investigated in quiescent air to simulate the take-off condition.

SYMBOLS

The following symbols are used in this report:

A area

h height of boundary-layer-removal scoop above flat plate

m mass flow

M Mach number

P total pressure

R inlet radius (measured from center line of spike to lip)

V velocity at any point

x lineal distance (parallel to plate)

y normal distance from plate surface

δ boundary-layer thickness, distance from surface to point in boundary layer where velocity is equal to 0.99 of free-stream velocity

Subscripts:

0 free-stream condition

1 actual conditions 1/2 inch upstream of spike tip

2 actual conditions at exit of diffuser or boundary-layer scoop

S boundary-layer scoop

C choking condition

D inlet

T throat

APPARATUS AND PROCEDURE

Model and Instrumentation

The side inlet (fig. 1) consisting of half of an axially symmetric 50°-conical-spike inlet mounted on a flat plate was alined at zero angle of attack and zero yaw with the local stream (except for slight flow angularity caused by boundary-layer growth). The subsonic portion of the diffuser was faired into a cylindrical combustion chamber with its axis displaced inboard of the spike axis. Boundary layer which developed on the plate was removed upstream of the inlet by a ram-type scoop. The inlet diffuser and boundary-layer-removal systems formed an integral unit which could be moved relative to the flat plate by means of spacers so as to vary the height of the boundary-layer scoop. Variation of the initial boundary layer was accomplished by changing the length of flat plate upstream of the inlet (8.5, 11.5, and 14.5 in.).

Significant design details of the side-inlet configuration including a cross section of the engine and boundary-layer systems with instrumentation are presented in figure 2(a).

Engine-induction system. - The 50°-conical-spike supersonic diffuser was designed for all external compression. The shock wave originating at the apex of the cone theoretically passes just upstream of the cowling lip and results in approximately 7.8-percent mass-flow spillage with the diffuser operating supercritically. The angle between the interior cowl surface at the lip and the cone axis was made equal to the flow deflection angle through the conical shock while the cowl-lip included angle was kept sufficiently small to preclude shock detachment. Details of the internal area distribution and contours of the subsonic diffuser are presented in figure 2(b).

A 40-tube pitot-static rake (shown in reference 1) was located 1/2 diameter downstream of the exit of the subsonic diffuser as indicated in figure 2(a) to determine the total-pressure recovery and flow distribution. The subsonic portion of the diffuser discharged into a section of pipe containing a standard A.S.M.E. orifice plate which was used to measure the engine mass flow and which in turn discharged into the tunnel subsonic diffuser (fig. 3).

Boundary-layer-removal system. - The boundary-layer scoop was of a simple ram type with straight leading edge located at the tip of the spike. Immediately downstream of the entrance, the passage diverged to an included angle of 1.5°. At a distance 1.45 inches from the entrance a sudden increase occurred in the axial area variation as a result of the mechanical design used to make the scoop height variable.

The downstream portion of the duct developed into a circular cross section at the end of which was located a 17-tube pitot rake to determine the total-pressure recovery. The boundary-layer air was ducted outside the tunnel and through a rotameter system to determine the scoop mass flow and subsequently was discharged back into the tunnel test section as a means of obtaining low back pressure (fig. 3). No external pump was used in the boundary-layer-scoop system.

Several alternative boundary-layer-removal systems were briefly investigated and are pictured in figure 4. The first of these systems (fig. 4(b)) simulated the original ram-type scoop (fig. 4(a)) operating at zero mass flow but the sides of the scoop were cut back to a distance of 1.082 inlet radius downstream of the cowling lip. Two widths of splitter plate were investigated. The second configuration (fig. 4(c)) also simulated a ram-type scoop operating at zero mass flow but with the leading edge swept to the inlet lip. The third configuration consisted of the side inlet with no removal of the initial boundary layer upstream

of the inlet but with the inlet cowling cut away in the corners as indicated in figure 4(d). The cut out length was kept constant at one inlet radius while the height was varied.

Boundary-layer variation and measurement. - The boundary-layer thickness upstream of the inlet was varied with three different plate lengths which resulted in initial boundary-layer thicknesses (based on $V/V_0 = 0.99$) of 0.140, 0.188, and 0.225 inch. In order to insure a fully developed turbulent boundary layer, roughness was added to the flat plate at a distance of 1/2 inch from the leading edge. This roughness consisted of a 1/4-inch strip of 180 carborundum dust sprinkled lightly on wet lacquer. Boundary-layer profiles 1/2 inch upstream of the inlet (station 1) were measured with four remote controlled pitot tubes spaced as indicated in figure 5. To determine whether the initial boundary layer was affected by the presence of the model, surveys were made at station 1 on an unbroken flat plate. No effect could be measured. Static pressures were measured on the plate in the planes of the surveys and were assumed constant throughout the boundary layer. In addition to obtaining the initial boundary-layer profiles, this instrumentation was utilized to determine the free-stream Mach number upstream of the inlets. After initially determining this information, the boundary-layer probes were removed for the remainder of the investigation.

The nondimensional boundary-layer velocity profiles obtained at each spanwise station for the three plate lengths are presented in figure 5. A mean curve is faired through the data which was assumed to be the profile for all calculations involving the initial boundary layer. The initial boundary-layer-thickness parameters δ/R (ratio of initial boundary-layer thickness to inlet radius) were 0.093, 0.125, and 0.150.

Test Conditions and Procedure

The investigation was conducted in the 18- by 18-inch supersonic wind tunnel at the NACA Lewis laboratory. The Mach number upstream of the inlet determined from local total and static pressures was 1.88 which was considered to be the free-stream Mach number. Test-section total temperature and pressure were approximately 150° F and atmospheric, respectively, which resulted in a Reynolds number of approximately 3.24×10^6 per foot. The dewpoint was maintained within the range of -20° to -5° F.

For each of the three initial boundary-layer-thickness parameters δ/R, the scoop height was varied from zero to a value greater than the boundary-layer thickness. The engine mass flow was varied for each scoop height and for various outlet area settings of the boundary-layer duct.

To simulate the take-off condition, the inlet was also investigated in quiescent air for a range of engine mass flows up to the choking value. For these tests the boundary-layer scoop was set at a height of 0.093 times the inlet radius but did not pass any air.

In addition to steady schlieren photographs of the flow in the vicinity of the inlet, high-speed motion pictures were taken. Pressures were recorded on tetrabromoethane multimanometer boards.

DISCUSSION OF RESULTS

The pressure-recovery and mass-flow characteristics of the main inlet and boundary-layer scoop are referenced to conditions immediately upstream of the inlet as determined by the aforementioned boundary-layer surveys. Thus, for example, at an inlet mass-flow ratio $m_D/m_{1,D}$ of 1, the inlet is capturing the maximum amount of mass flow that is possible in the given flow field. Similarly at an inlet total-pressure recovery $P_{2,D}/P_{1,D}$ of 1, the inlet is recovering all of the total pressure available upstream of the inlet in this maximum stream tube.

Conditions upstream of the inlet represent a defect of mass flow and total pressure from the free-stream conditions. These defects are best represented by (1) the ratio of the average total pressure in the actual maximum stream tube that could be captured by inlet or boundary-layer scoop to the free-stream total pressure and (2) the ratio of the maximum mass flow possible to the mass flow that an equal-area stream tube would pass in the free stream. Knowledge of these ratios quickly enables the present data to be referenced to free-stream conditions if desired. The variations of average mass-flow and total-pressure ratios upstream of the inlet only and upstream of the inlet plus the boundary-layer scoop for various settings of the scoop height and for the three thicknesses of initial boundary layer are presented in figures 6(a) and 6(b). With no removal of the thickest boundary layer ($h/\delta = 0$, $\delta/R = 0.15$), the maximum available pressure recovery and mass-flow ratio of the inlet were still 0.95. Figure 6(c) presents similar plots for the boundary-layer scoop.

Visual Flow Observations

Schlieren photographs of the inlet operating at peak pressure recovery for several values of boundary-layer-scoop-height parameter h/δ less than 1 are presented in figure 7(a). The peak pressure recoveries correspond to maximum flow in the boundary-layer scoop. Figure 7(b) shows the inlet operating at two different scoop heights greater than the boundary-layer thickness. At these scoop heights the peak pressure recovery point was obtained with a slightly subcritical

mass-flow ratio in the boundary-layer scoop rather than at maximum flow as will be discussed later. The shock patterns were noticeably different.

The small shock wave originating on the plate just upstream of the boundary-layer scoop arose from air leakage through the very small (0.020 in.) instrumentation holes in the plate. The apparently strong oblique shock waves upstream of the inlet originated at the strip of roughness at the plate leading edge and at the attachment joint of the plate extension. These waves do not affect the results of these tests.

In contrast to nose installations, the spike-type diffuser as a side inlet exhibited various types of unsteady operation. The approximate buzz patterns are indicated in figure 8. Figure 8(a) shows a steady shock pattern whereas figures 8(b) to 8(e) indicate the extremities of the buzz patterns obtained. With complete removal of the boundary layer, the inlet buzz was of the usual form for subcritical nose-inlet operation, that is, with the shock pattern oscillating from inside the inlet to the tip of the spike (fig. 8(b)). If some boundary layer was spilled into the inlet either by reduced scoop height or mass-flow ratio, this subcritical shock oscillation extended out onto the flat plate upstream of the inlet for a distance as great as several inlet diameters (fig. 8(c)). Accompanying this shock travel was separation of the boundary layer on the plate with a resulting oscillation of the inlet and scoop mass flows. When the boundary-layer scoop was operating subcritically and the inlet supercritically, another type of buzz was encountered. In this case the high-speed photographs showed a slight fore and aft high-frequency oscillation of the oblique shock wave upstream of the boundary-layer scoop (fig. 8(d)). A mixed buzz condition occurred when the inlet was operating very near peak pressure recovery with the boundary-layer scoop operating subcritically. In this condition the oscillating oblique shock upstream of the boundary-layer scoop apparently caused the inlet shock to oscillate along the length of the spike as shown in figure 8(e).

Main Inlet Performance

The basic inlet performance data for each setting of inlet and scoop mass-flow ratio consisted of total and static pressure distributions at the end of the subsonic portion of the diffuser. Typical distributions in the form of total pressure and Mach number contour maps are presented in figure 9. The cases considered are the peak pressure recovery conditions for three settings of the boundary-layer-scoop height with maximum mass flow through the boundary-layer scoop. In general, the point of maximum local total-pressure recovery was shifted outboard from the axis of the discharge duct. This condition became more pronounced as the boundary-layer-scoop height was increased and

was accompanied by strong Mach number gradients. For large scoop heights, a considerable region of separated flow was present.

The average total-pressure recoveries obtained were based on an area weighting technique. Even with the poor pressure distribution of figure 9(c), the maximum spread in pressure recovery among various averaging techniques was approximately 1.8 percent due to the relatively low discharge velocities.

Typical variations of inlet pressure recovery with inlet mass-flow ratio are presented in figure 10 for a single value of initial boundary-layer-thickness parameter δ/R of 0.093. Data for values of scoop height parameter h/δ of 0 to 1.571 are presented. For each scoop height setting, the pressure-recovery variations for a range of outlet area settings on the boundary-layer scoop are shown. In the supercritical range of inlet operation, the fixed outlet on the boundary-layer scoop corresponded (for a given scoop height) to a fixed boundary-layer mass-flow ratio with which the individual curves are labeled. In certain ranges of subcritical inlet operation, however, the inlet shock configuration influenced the boundary-layer flow as illustrated in figure 10(c) where the subcritical boundary-layer-scoop mass-flow ratios are labeled. (Where a maximum scoop or inlet mass-flow ratio greater than 1 is indicated, some inaccuracy probably occurred in either measurement of the mass flow or estimation of the maximum possible mass flow. The error in estimating maximum mass flow could arise from deflection of the scoop lip in the case of the boundary-layer scoop.)

In general for large values of boundary-layer-scoop mass-flow ratio, the pressure recovery mass-flow characteristics were of the usual form for a spike-type diffuser. These characteristics indicated peak pressure recovery at a slightly subcritical inlet mass-flow ratio which was followed by a severe reduction in pressure recovery with further reduction in mass-flow ratio as a result of diffuser buzz. Reduction of the boundary-layer-scoop mass-flow ratio to values less than unity had three effects as shown in figure 10: (1) the supercritical inlet mass-flow ratio was reduced, (2) the peak pressure recovery was reduced, and (3) the peak pressure recovery was shifted to lower values of inlet mass-flow ratio. The regions of unsteady operation are shown as dotted lines in the figure. (With supercritical inlet operation the oscillations were small, but for subcritical inlet operation the oscillations were frequently very large; hence, the manometer averages are somewhat questionable.)

An exception to these trends occurred when the boundary-layer-scoop height exceeded the boundary-layer thickness. In this case the highest pressure recoveries were obtained with a boundary-layer-scoop mass-flow ratio of slightly less than maximum. With a boundary-layer thickness corresponding to δ/R of 0.093 and h/δ of 1.571, the increase in

recovery as the scoop mass-flow ratio was reduced was not pronounced; this increase can be qualitatively explained by an observed reduction in the inlet internal separation when some boundary layer is spilled into the inlet. For h/δ of 1.250, however, where the greatest effect was observed, the amount of internal separation at the end of the subsonic diffuser did not appreciably vary with the slight change in boundary-layer-scoop mass-flow ratio (0.88 to 1.03).

A summary plot of the peak total-pressure recovery $P_{2,D}/P_{1,D}$ as a function of boundary-layer-scoop-height parameter h/δ for various boundary-layer-scoop mass-flow ratios is shown in figure 11 for δ/R of 0.093. With complete removal of the initial boundary layer, the side inlet yielded a total-pressure recovery of approximately 89 percent and was comparable to a nose inlet. The theoretical shock recovery was approximately 94 percent which indicates subsonic diffuser recovery of approximately 95 percent. Allowing the entire initial boundary layer to flow into the inlet lowered the inlet total-pressure recovery to approximately 70 percent although the initial defect in total pressure in the boundary layer did not greatly affect the average total pressure upstream of the inlet.

Pitot surveys of the inlet throat indicated that the shock losses agreed with the theoretical losses; hence, large additional losses in total pressure occurred in the subsonic diffuser. Application of a boundary-layer-control system within the subsonic diffuser by such schemes as vortex generators or self-energized internal boundary-layer removal may be effective in reducing these losses.

The inlet was particularly sensitive to subcritical scoop operation for large values of h/δ. In such cases, for values of boundary-layer-scoop mass-flow ratio somewhat less than the optimum, unstable operation of the scoop and subsequently the inlet reduced the inlet pressure recovery markedly. In figure 11 for values of scoop height below those where buzz is encountered, the variations of peak pressure recovery with scoop-height parameter for subcritical scoop operation may be predicted from the variation with supercritical scoop operation by assuming that the inlet pressure recovery is only a function of the boundary-layer mass flow that enters it and not of the scoop height. The amount of boundary-layer mass flow that enters the inlet is defined by the height of the stagnation streamline (see sketch on fig. 11). Thus with subcritical scoop operation, the inlet pressure recovery is assumed equal to that obtained with supercritical operation of a scoop of height equal to the height of the stagnation streamline under consideration.

The variations of peak total-pressure recovery with boundary-layer-scoop-height parameter for the three values of initial boundary-layer-thickness parameter are shown in figure 12. These data were obtained at boundary-layer mass-flow ratios that were optimum with respect to inlet

pressure recovery. Only a small initial spread in the data was observed at zero scoop height despite the difference in initial boundary-layer thickness which indicates that all three thicknesses were sufficiently large to destroy the subsonic diffuser flow. With most of the boundary layer removed, the pressure recovery curves were comparable. In this region a single rough fairing is shown as well as three individual fairings based on an unexplained tendency towards a slight peaking at values of scoop height approximately equal to the boundary-layer thickness.

The point of peak pressure recovery is not necessarily the most desirable point at which to operate a supersonic diffuser when this peak is considerably subcritical. For this reason the curves of pressure recovery as a function of inlet mass-flow ratio are presented in figure 13 for each initial boundary-layer thickness and scoop height to supplement figures 10 and 11. Boundary-layer-scoop mass-flow ratio was maximum or slightly less as indicated. The optimum operating point is a function of the particular inlet-engine combination under consideration.

Inlet Performance with Modified Boundary-Layer Control

The sensitivity of the inlet pressure recovery to subcritical operation of the boundary-layer scoop has already been discussed. Several alternative boundary-layer-removal systems (fig. 4) designed to eliminate this spread between the zero and maximum scoop mass-flow curves were briefly investigated.

In the first configuration (fig. 4(b)), the sides of the original ram scoop were removed so that any throttling of the boundary-layer duct would result in spillage of the flow to the sides rather than over the scoop and into the inlet. This configuration was only investigated for the case of 100-percent spillage. The inlet pressure recovery plotted against mass flow with this configuration and with the same general configuration with a widened splitter plate are shown in figure 14(a) for two values of scoop height. The best pressure recovery was obtained with a scoop height equal to the boundary-layer thickness and was approximately 8 percent below what might be expected if the boundary layer were ducted off as with the original ram-type scoop. This discrepancy apparently resulted from a shock which was observed in schlieren photographs to stand upstream of the scoop. The shock would be expected from the blunt-body-type duct blockage used for these tests. Presumably, if the blockage under the plate were moved far enough downstream, the inlet pressure recovery should approach the ram-type scoop value. Also use of a low angle wedge under the splitter plate to "plow" the boundary

layer aside should be effective and may prove advantageous in cases where there is no practical need, such as for cooling purposes, to utilize the boundary-layer air.

The second configuration (fig. 4(c)) investigated simulated a ram-type scoop with a leading edge swept from the cone tip to the inlet lip. Again the case of zero scoop mass flow was considered. The best pressure recovery of 85 percent (fig. 14(b)) was obtained with a scoop height equal to the boundary-layer thickness and was only 4 percent less than what might be expected with the scoop passing maximum mass flow.

The third configuration (fig. 4(d)) departed from the previous approaches which considered removal of the boundary layer upstream of the inlet. Pitot-pressure surveys at the throat of the inlet indicated that most of the initial boundary layer flowed around the spike and filled the corners of the annular throat. Because this pile up of low energy air was located close to the cowling, it appeared that cutting slots in the cowl corners might be more effective in removing the boundary layer than they were on the ramp-type inlets of reference 2. Accordingly, the ram scoop was eliminated and slots one inlet radius long and of several heights were investigated. The results, presented in figure 14(c), indicated a pressure recovery of 86 percent with a slot height of $1\frac{1}{2}$ times the initial boundary-layer thickness. (Additional slot height or length might still further have improved the performance as might locating scoops in the corners of the annular throat rather than merely slotting the cowling.) This recovery was obtained at an inlet mass-flow ratio of 0.845 which was slightly less than in the case of the ram-type scoop of $h/\delta = 0.9$ where the inlet captured 0.9 of the maximum possible mass flow through the inlet plus boundary-layer scoop.

A summary plot of the results is presented in figure 15 with peak pressure recovery as a function of h/δ where h is also the slot height in the case of the slotted cowl.

Nonuniform Initial Boundary Layer

Actual installation of an inlet on an aircraft fuselage at angle of attack may result in a nonuniform boundary layer upstream of the inlet. To simulate this condition the original configuration with ram-type boundary-layer scoop was investigated on a flat plate with a swept leading edge. The swept leading edge caused a nearly linear spanwise variation of boundary-layer thickness upstream of the scoop as indicated in the sketch of figure 16. This figure presents the variation of peak pressure recovery with the boundary-layer-scoop-height parameter h/δ where δ is taken as the maximum δ upstream of the scoop. This curve is nearly coincident with the original variation with uniform boundary

[redacted]

layer with approximately the same value of δ which indicates the maximum thickness of the initial boundary layer to be a significant parameter in determining the internal losses.

Boundary-Layer-Scoop Performance

Because of the discontinuity in the axial area variation of the boundary-layer ducting, the pressure recoveries obtained in the boundary-layer system were probably lower than could be achieved by careful design. The pressure recoveries obtained with the system used in this investigation are considered of general interest, however, and are presented in figure 17 as a function of boundary-layer-scoop mass-flow ratio for various scoop heights. The main inlet was operating supercritically for this data. Figure 17(a) references the recovered pressure to the average total pressure upstream of the scoop whereas figure 17(b) references to free-stream total pressure. As would be expected the low scoop heights yielded the highest recoveries referenced to conditions upstream of the scoop as a result of the low initial average Mach numbers and yielded the lowest recoveries referenced to stream conditions.

The amount of boundary layer handled as a percentage of maximum inlet mass flow is presented as a function of h/δ in figure 18. As would be expected the amount of air handled to obtain peak inlet pressure recovery increases as the boundary-layer thickness upstream of the inlet increases. At a value of h/δ of 1.00, for example, the quantities removed were 9.8, 13.0, and 14.5 percent of the inlet mass flow for values of δ/R of 0.093, 0.125, and 0.150, respectively. This range of 10 to 15 percent of inlet mass flow is typical of that required for engine cooling purposes.

The optimum amount of boundary-layer removal with the ram-type scoop as well as the various other systems investigated is a function not only of the corresponding inlet and hence engine performance but also of the cost in drag of handling the boundary-layer air. Consideration of the drag is beyond the scoop of the present investigation.

Inlet Performance at Take-Off

In the application of air inlets to aircraft, it is desirable that the inlet operate satisfactorily over the entire flight range from zero to maximum flight speed. Accordingly, the inlet was investigated at the take-off condition of zero forward speed. Pressure recoveries were determined over the range of mass flows up to maximum and are presented in figure 19 as a function of inlet choking mass-flow ratio $m_D/m_{D,C}$

where $m_{D,C}$ is the theoretical mass flow which could be captured with a choked minimum geometric throat area. The pressure recovery decreased appreciably as the mass flow approached a limiting value of 80 percent of the theoretical maximum. This limit probably resulted from internal separation of the flow due to the sharp lip. The data indicate that an inlet with a sharp lip is not satisfactory for take-off unless the throat velocity is kept very low by use of blow-in doors or some similar procedure.

SUMMARY OF RESULTS

An experimental investigation at Mach number 1.88 of the performance of a spike-type side inlet with boundary-layer removal yielded the following results:

1. With complete removal of the initial boundary layer upstream of the inlet by means of a ram-type scoop, the side inlet yielded an inlet total-pressure recovery of approximately 89 percent which indicated a subsonic diffuser recovery of approximately 95 percent and was comparable to nose-inlet performance.

2. Allowing the initial boundary layer to flow into the inlet lowered the inlet total-pressure recovery to approximately 70 percent although the initial defect in total pressure in the boundary layer did not greatly affect the average total pressure upstream of the inlet. Most of the additional losses were determined to occur in the subsonic diffuser, which suggests the application of internal boundary-layer control.

3. The inlet performance with a ram-type scoop was sensitive to the boundary-layer-scoop mass-flow ratio. Several alternative boundary-layer-removal systems were briefly investigated which greatly reduced this sensitivity.

4. The inlet was subject to large total-pressure losses when operating at zero forward velocity and high throat velocities.

Lewis Flight Propulsion Laboratory,
National Advisory Committee for Aeronautics,
Cleveland, Ohio.

REFERENCES

1. Hunczak, Henry R., and Kremzier, Emil J.: Characteristics of Perforated Diffusers at Free-Stream Mach Number 1.90. NACA RM E50B02, 1950.

2. Davis, Wallace F., and Goldstein, David L.: Experimental Investigation at Supersonic Speeds of Twin-Scoop Duct Inlets of Equal Area. II - Effects of Slots upon an Inlet Enclosing 61.5 Percent of the Maximum Circumference of the Forebody. NACA RM A8C11, 1948.

Figure 1. - Conical-spike diffuser mounted as side inlet in tunnel.

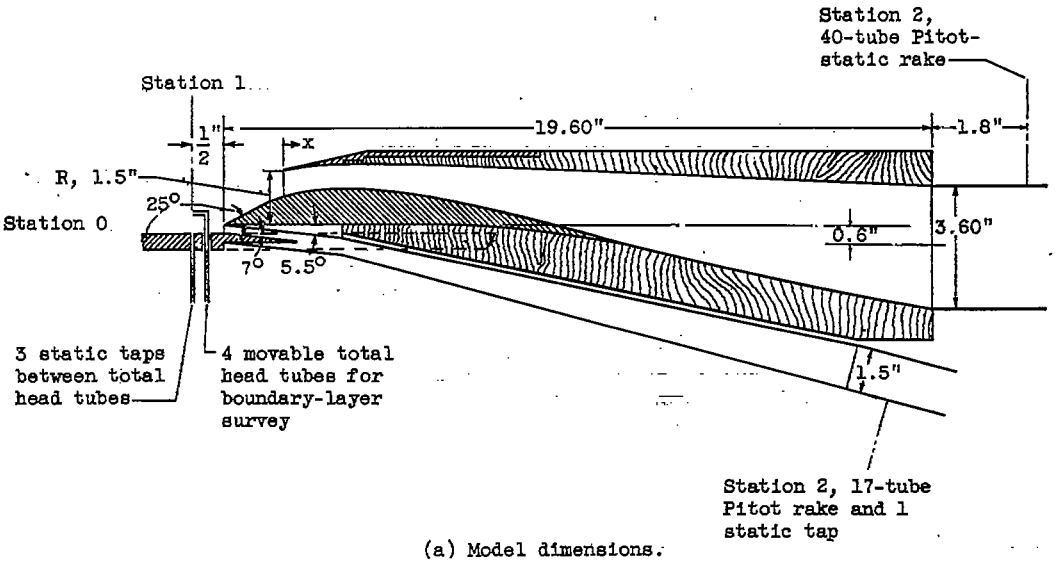

(a) Model dimensions.

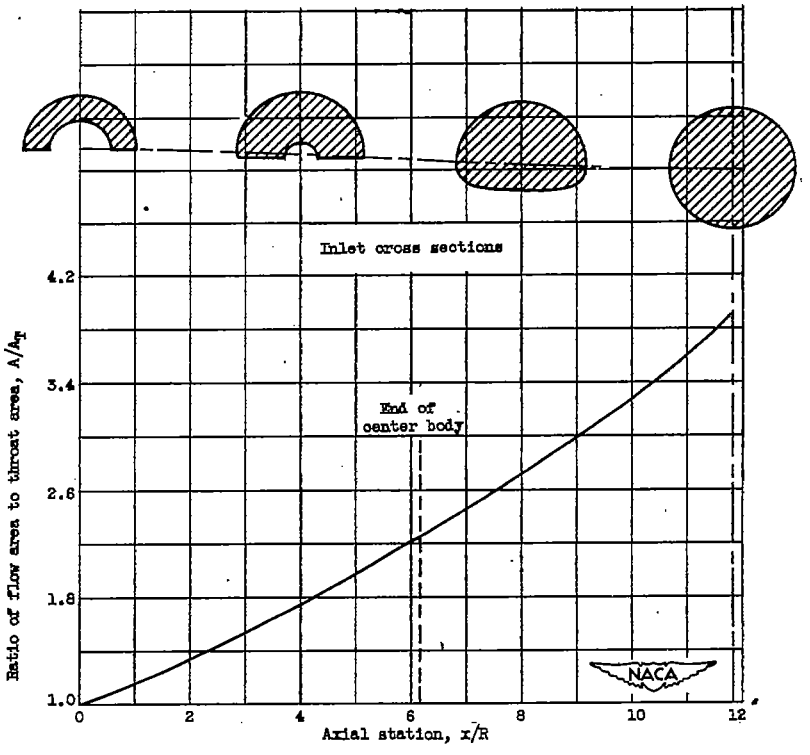

(b) Internal area variation.

Figure 2. - Dimensions and cross-section-area variations of side-inlet configuration.

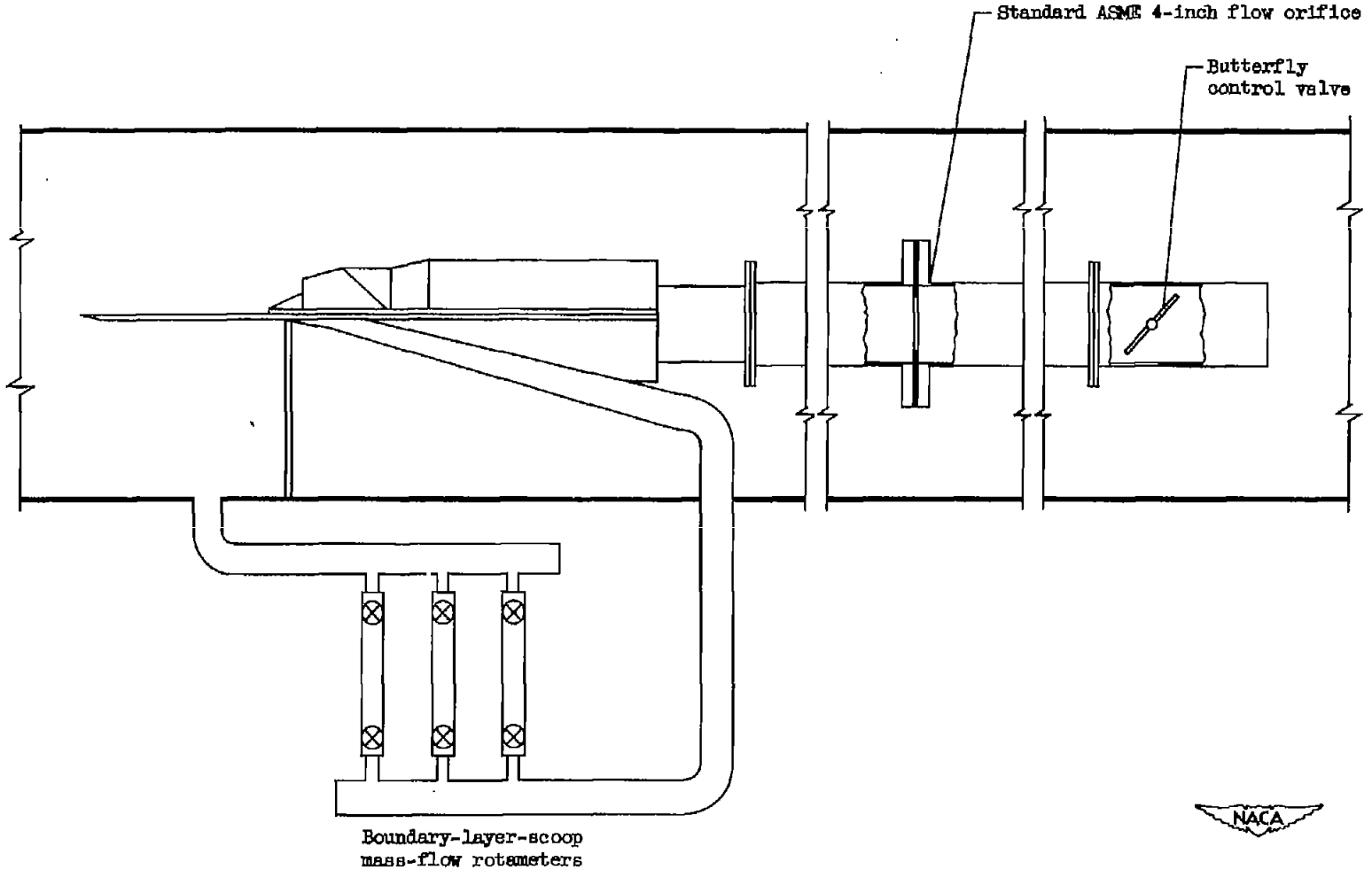

Figure 3. - Flow measuring instrumentation.

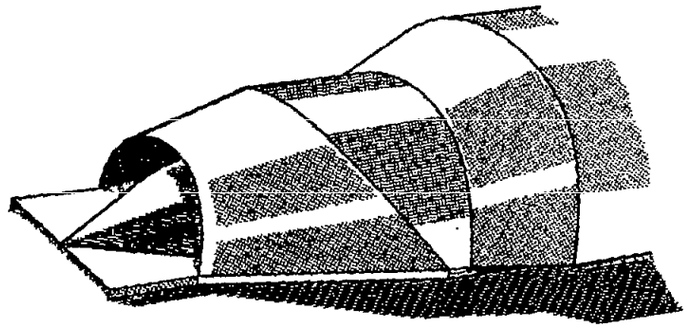

(a) Original ram-type scoop.

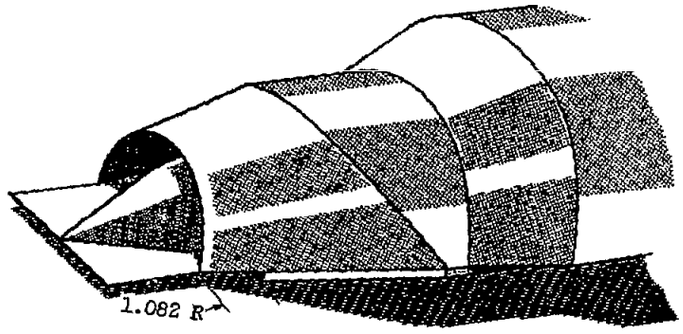

(b) Ram-type scoop with sides removed.

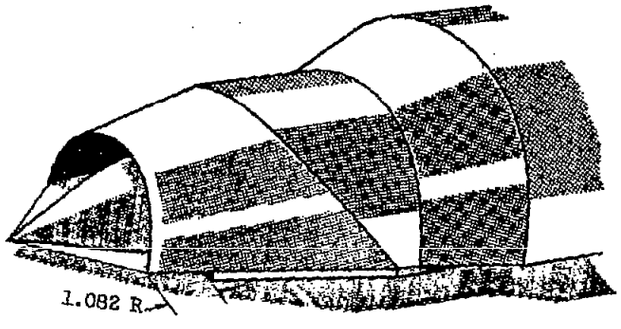

(c) Ram-type scoop with swept leading edge.

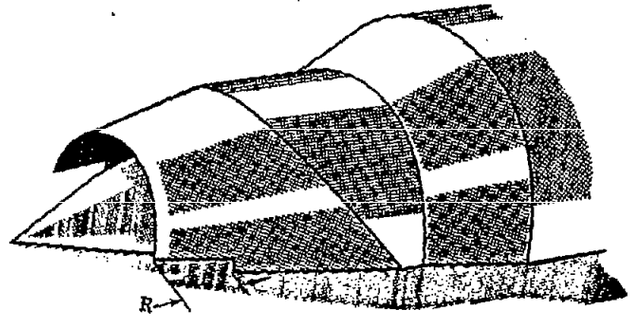

(d) No scoop; cowl slots.

Figure 4. - Several boundary-layer-removal systems.

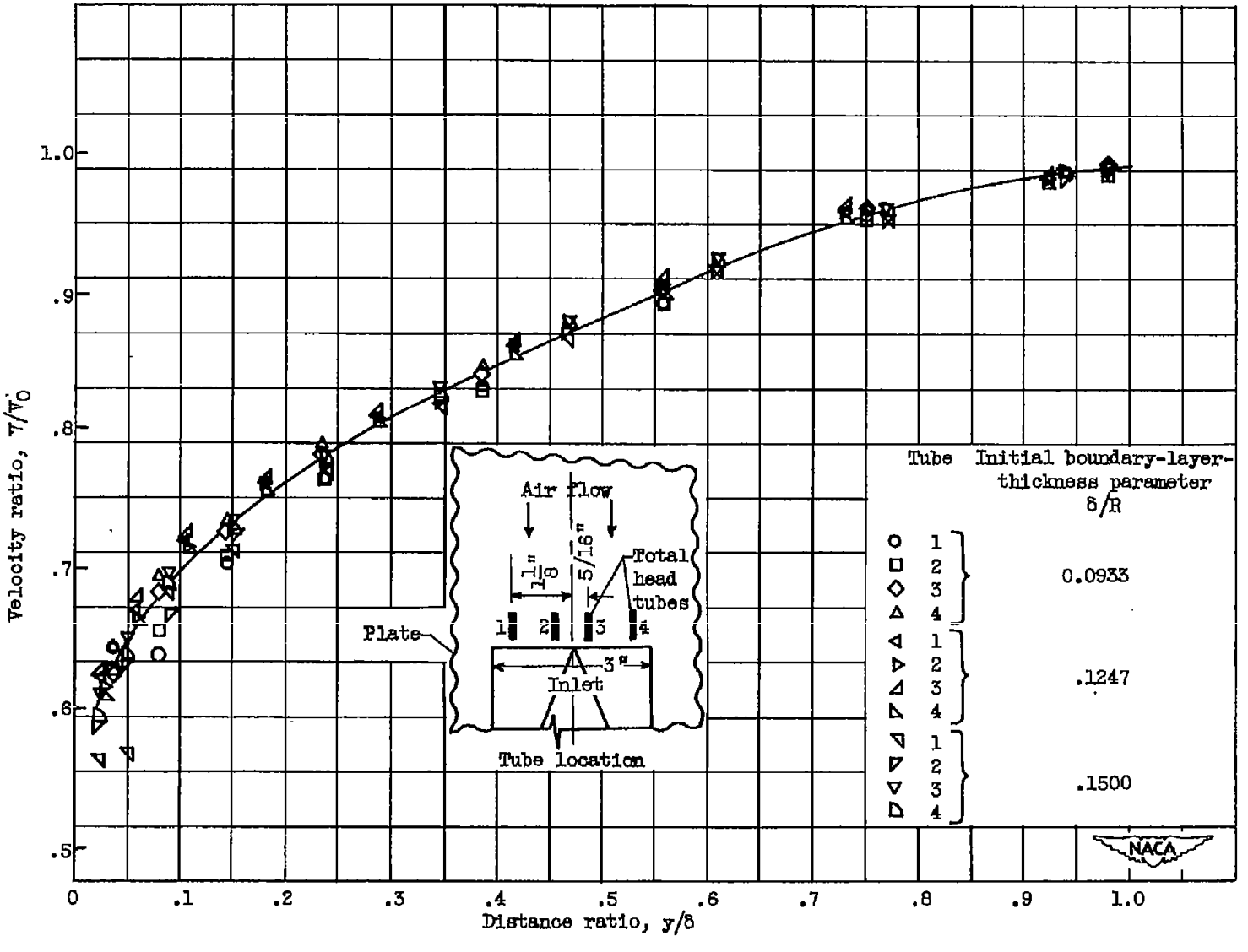

Figure 5. - Velocity profiles of the three initial boundary layers.

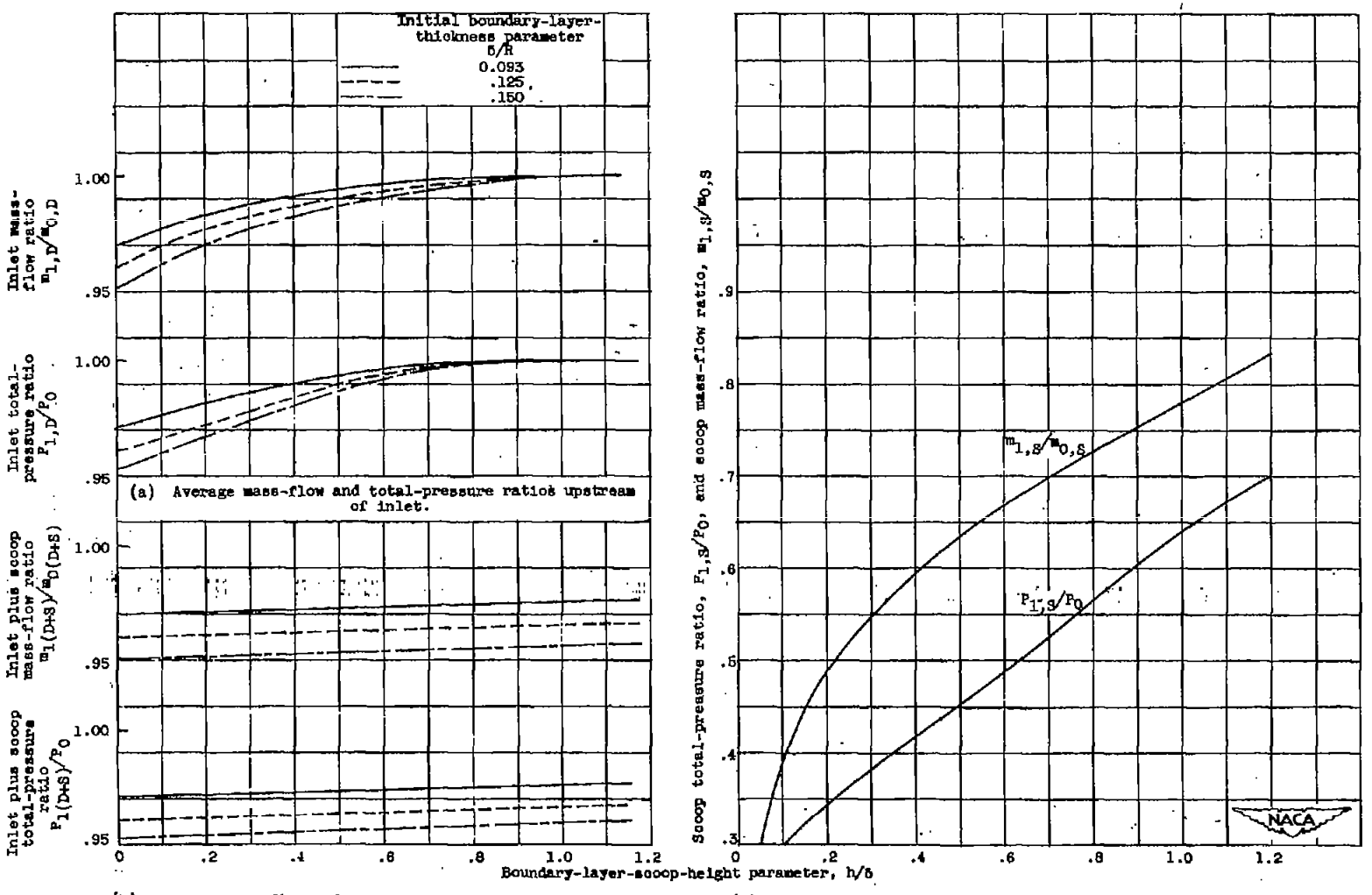

(a) Average mass-flow and total-pressure ratios upstream of inlet.

(b) Average mass-flow and total-pressure ratios upstream of combination of inlet plus boundary-layer scoop.

(c) Average mass-flow and total-pressure ratios upstream of boundary-layer scoop.

Figure 5. - Variation of average mass-flow and total-pressure ratios at station 1.

Boundary-layer-scoop-height parameter h/δ, 0 (no scoop); inlet total-pressure recovery $P_{2,D}/P_{1,D}$, 0.7060; inlet supercritical.

Boundary-layer-scoop-height parameter h/δ, 0.571; scoop mass-flow ratio $m_S/m_{1,S}$, 0.950 (max.); inlet total-pressure recovery $P_{2,D}/P_{1,D}$, 0.8157; inlet supercritical.

NACA C-27980

Boundary-layer-scoop-height parameter h/δ, 0.893; scoop mass-flow ratio $m_S/m_{1,S}$, 1.048 (max.); inlet total-pressure recovery $P_{2,D}/P_{1,D}$, 0.8905; inlet supercritical.

(a) Boundary-layer-scoop-height parameter h/δ, < 1.

Figure 7. - Steady schlieren photographs.

Boundary-layer-scoop-height parameter h/δ, 1.250; scoop mass-flow ratio $m_S/m_{1,S}$, 1.030 (max.); inlet total-pressure recovery $P_{2,D}/P_{1,D}$, 0.8306; inlet supercritical; scoop supercritical.

Boundary-layer-scoop-height parameter h/δ, 1.571; scoop mass-flow ratio $m_S/m_{1,S}$, 1.040 (max.); inlet total-pressure recovery $P_{2,D}/P_{1,D}$, 0.8695; inlet supercritical; scoop supercritical.

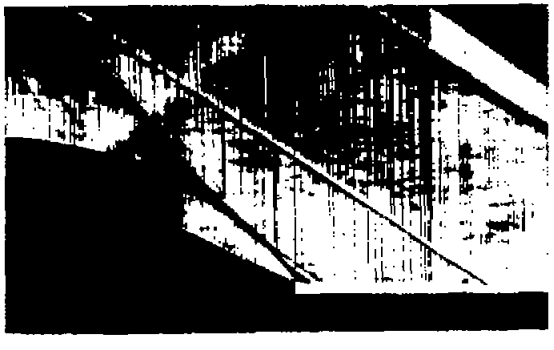

Boundary-layer-scoop-height parameter h/δ, 1.250; scoop-mass-flow ratio $m_S/m_{1,S}$, 0.760; inlet total-pressure recovery $P_{2,D}/P_{1,D}$, 0.8848; inlet supercritical; scoop subcritical.

Boundary-layer-scoop-height parameter h/δ, 1.571; scoop mass-flow ratio $m_S/m_{1,S}$, 0.851; inlet total-pressure recovery $P_{2,D}/P_{1,D}$, 0.8812; inlet supercritical; scoop subcritical.

NACA

C-27981

(b) Boundary-layer-scoop-height parameter h/δ, > 1.

Figure 7. - Concluded. Steady schlieren photographs.

(a) Steady flow pattern; boundary-layer-scoop-height parameter $h/\delta > 1$; scoop mass-flow ratio $m_s/m_{1,s}$, 1.0.

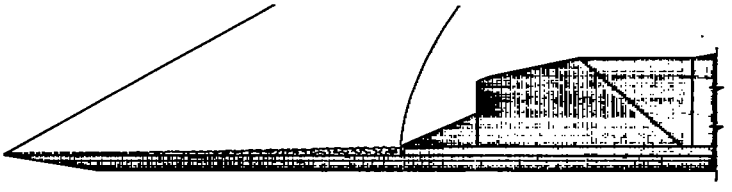

(b) Subcritical inlet flow; boundary-layer-scoop-height parameter $h/\delta > 1$; scoop mass-flow ratio $m_s/m_{1,s}$, 1.0.

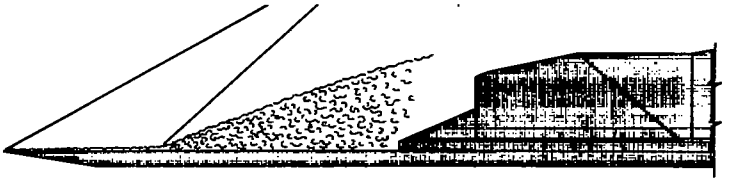

(c) Subcritical inlet flow; boundary-layer-scoop-height parameter $h/\delta > 1$; scoop mass-flow ratio $m_s/m_{1,s}$, 0.

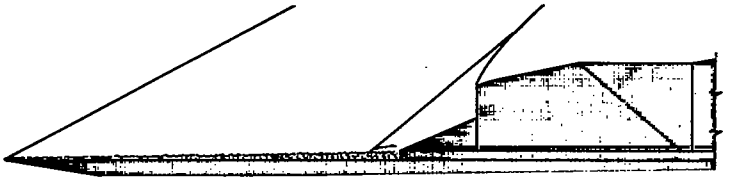

(d) Supercritical inlet flow; boundary-layer-scoop-height parameter $h/\delta > 1$; scoop mass-flow ratio $m_s/M_{1,s}$, 0.60.

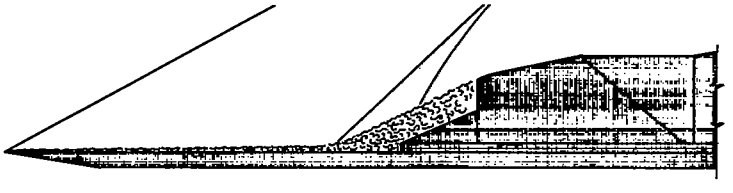

(e) Inlet oscillation induced by scoop; boundary-layer-scoop-height parameter $h/\delta > 1$, scoop mass-flow ratio $m_s/m_{1.s}$, 0.60.

Figure 8. - Various types of buzz patterns encountered.

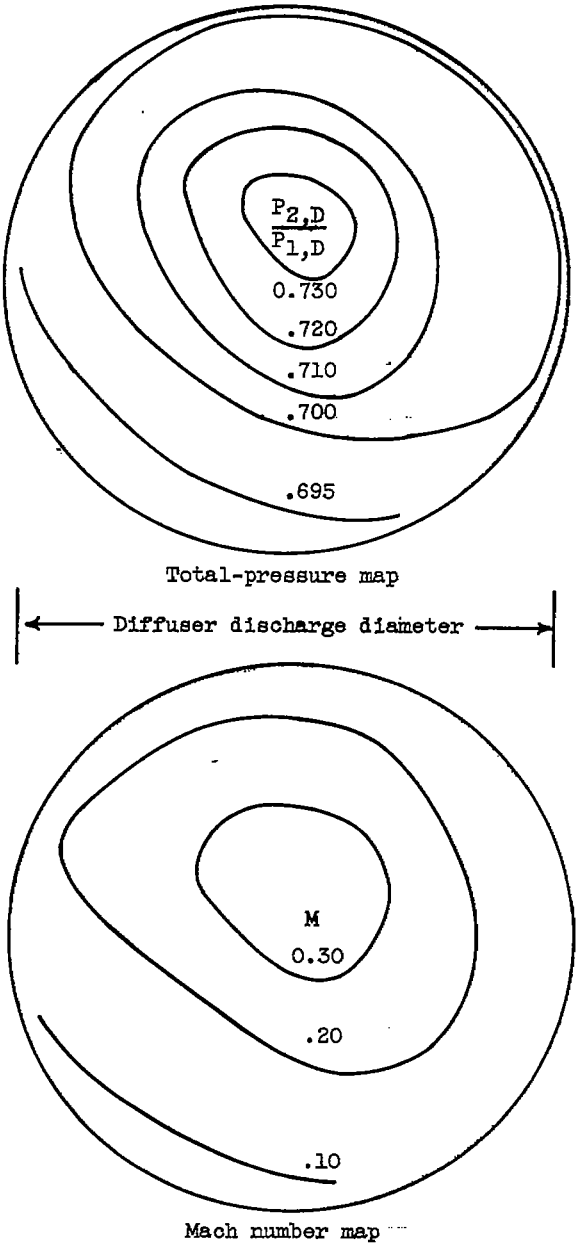

(a) Boundary-layer-scoop-height parameter $\bar{h}/\delta$, 0; $P_{2,D}/P_{1,D}$, 0.706.

Figure 9. - Total-pressure and Mach number contour maps at diffuser discharge.

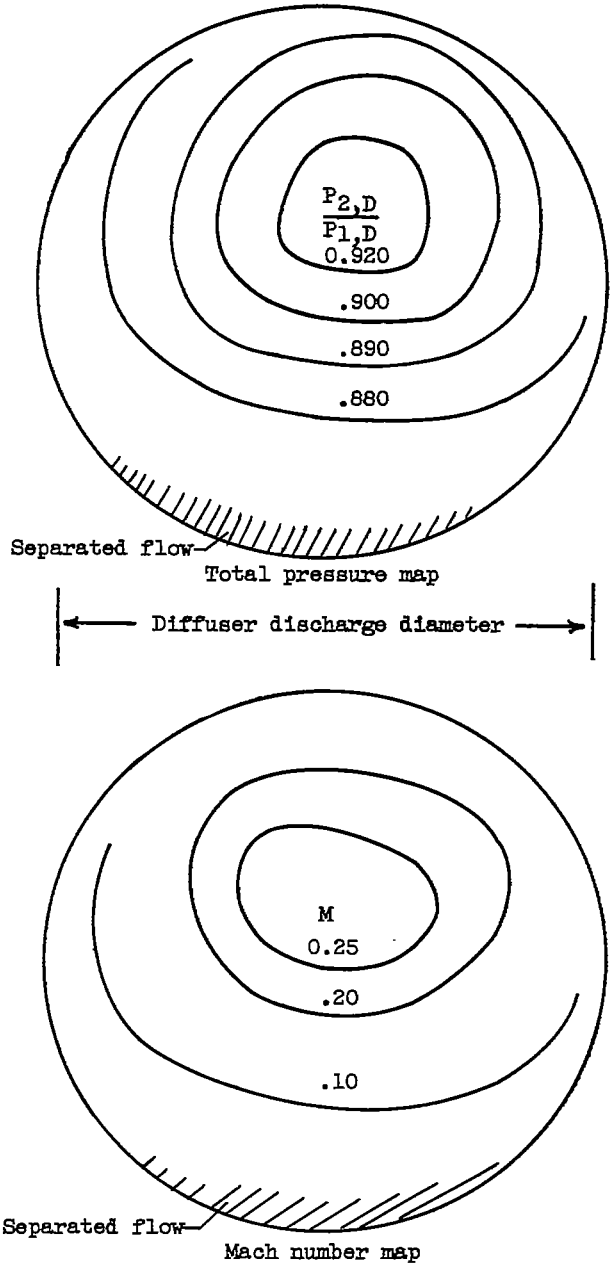

(b) Boundary-layer-scoop-height parameter h/δ, 0.893; $P_{2,D}/P_{1,D}$, 0.891.

Figure 9. - Continued. Total-pressure and Mach number contour maps at diffuser discharge.

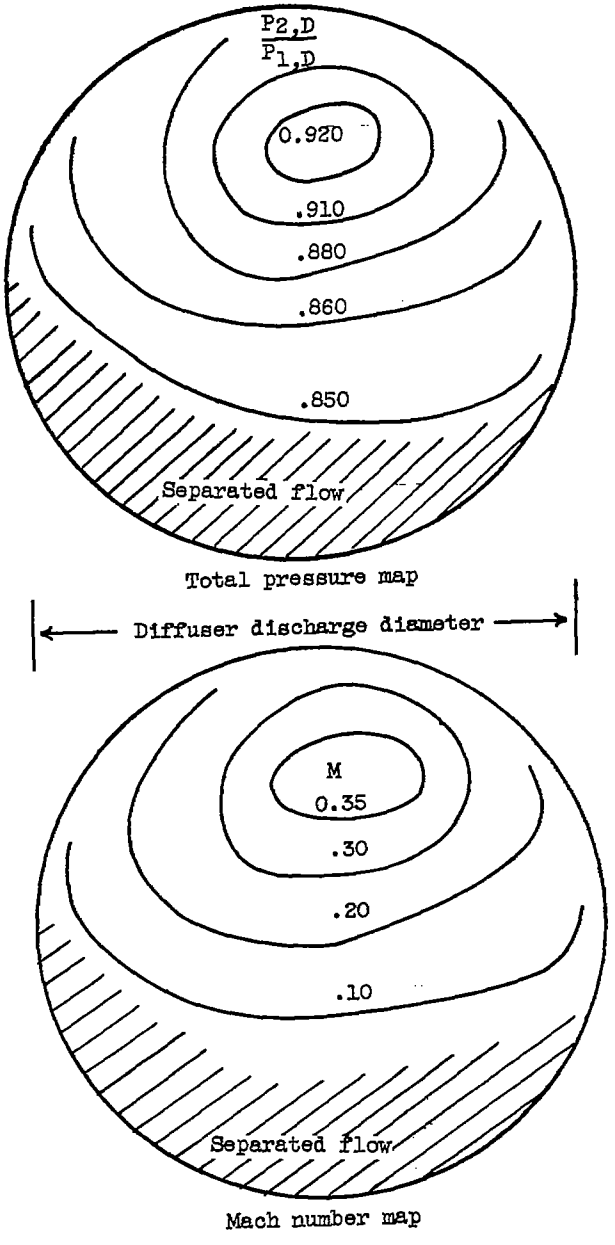

(c) Boundary-layer-scoop-height parameter h/δ, 1.571; $P_{2,D}/P_{1,D}$, 0.870.

Figure 9. - Concluded. Total-pressure and Mach number contour maps at diffuser discharge.

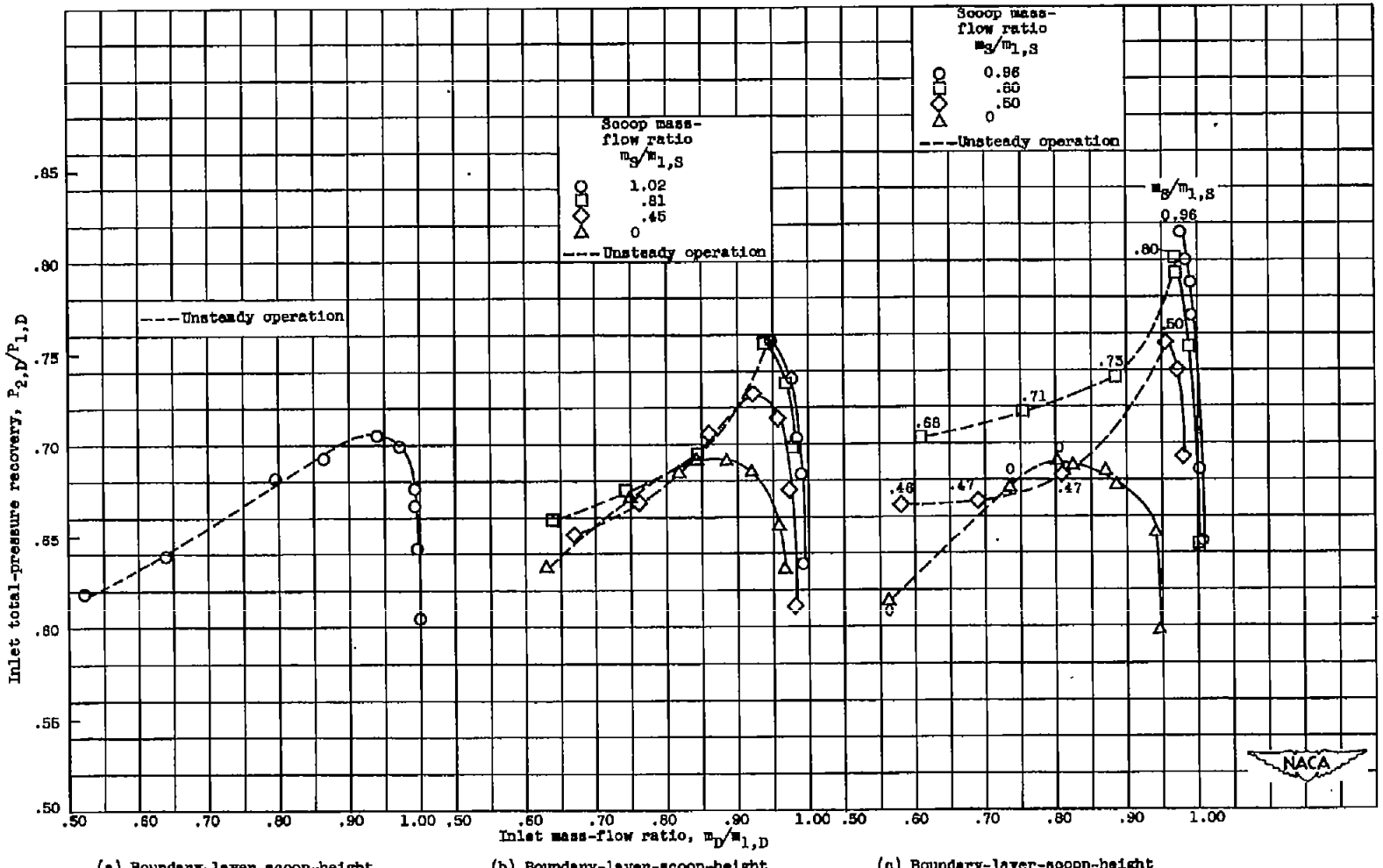

(a) Boundary-layer-scoop-height parameter h/δ, 0.

(b) Boundary-layer-scoop-height parameter h/δ, 0.235.

(c) Boundary-layer-scoop-height parameter h/δ, 0.571.

Figure 10. - Inlet pressure recovery as a function of inlet mass-flow ratio for various boundary-layer-scoop heights and mass-flow ratios and for a boundary-layer-thickness parameter of 0.083.

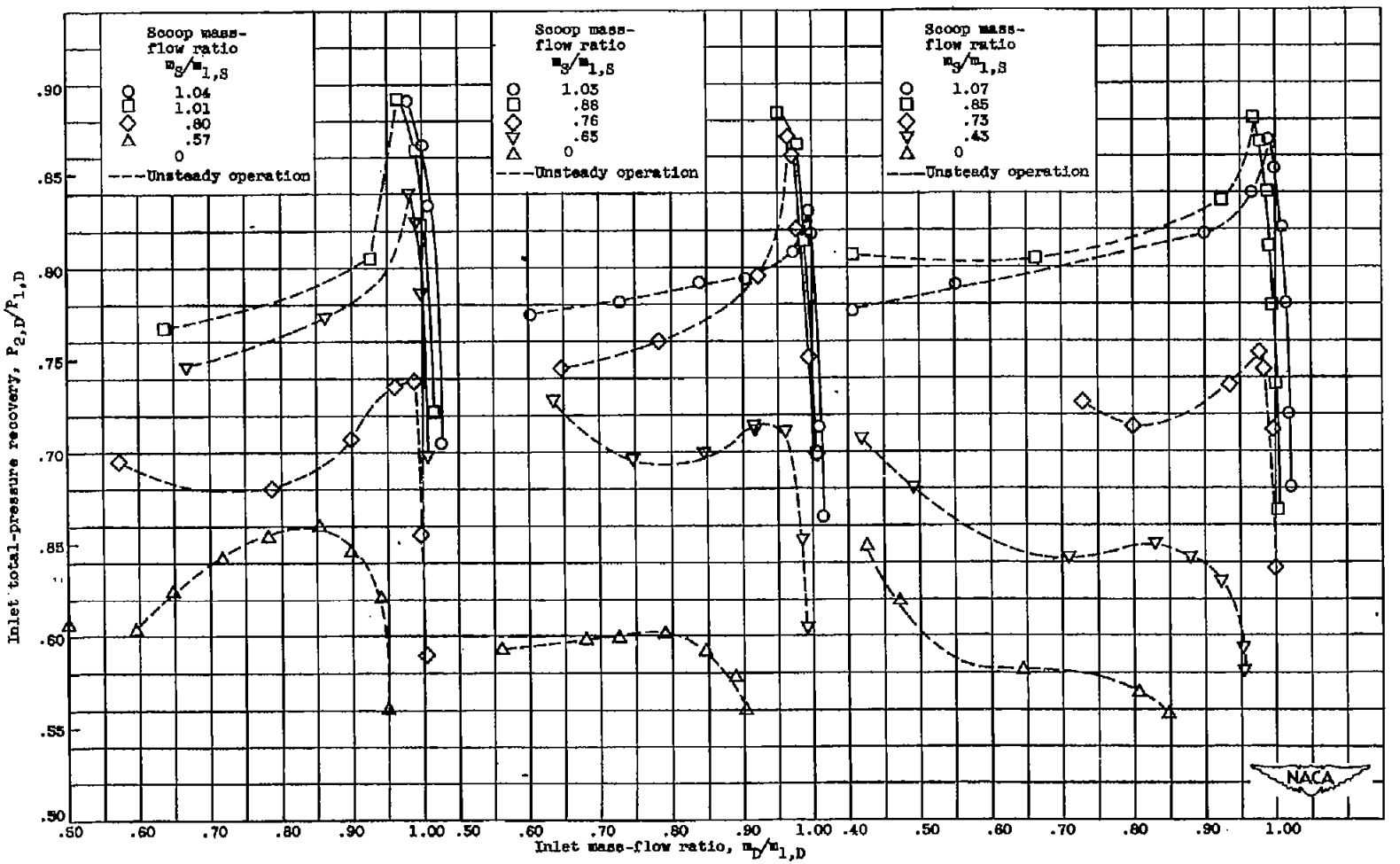

(d) Boundary-layer-scoop-height parameter h/δ, 0.893.

(e) Boundary-layer-scoop-height parameter h/δ, 1.250.

(f) Boundary-layer-scoop-height parameter h/δ, 1.571.

Figure 10. - Concluded. Inlet pressure recovery as a function of inlet mass-flow ratio for various boundary-layer-scoope heights and mass-flow ratios and for a boundary-layer-thickness parameter of 0.093.

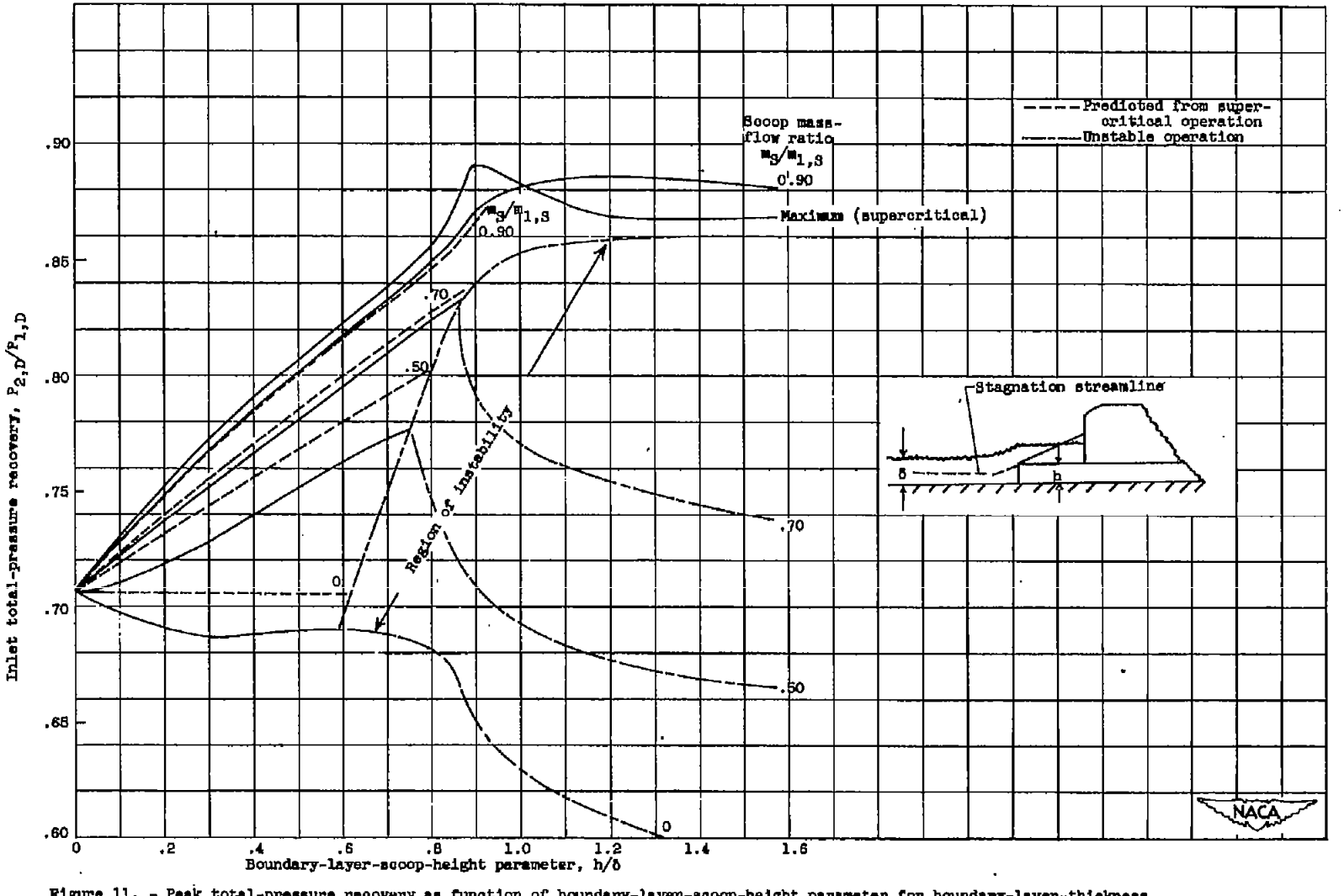

Figure 11. - Peak total-pressure recovery as function of boundary-layer-scoop-height parameter for boundary-layer-thickness parameter of 0.095.

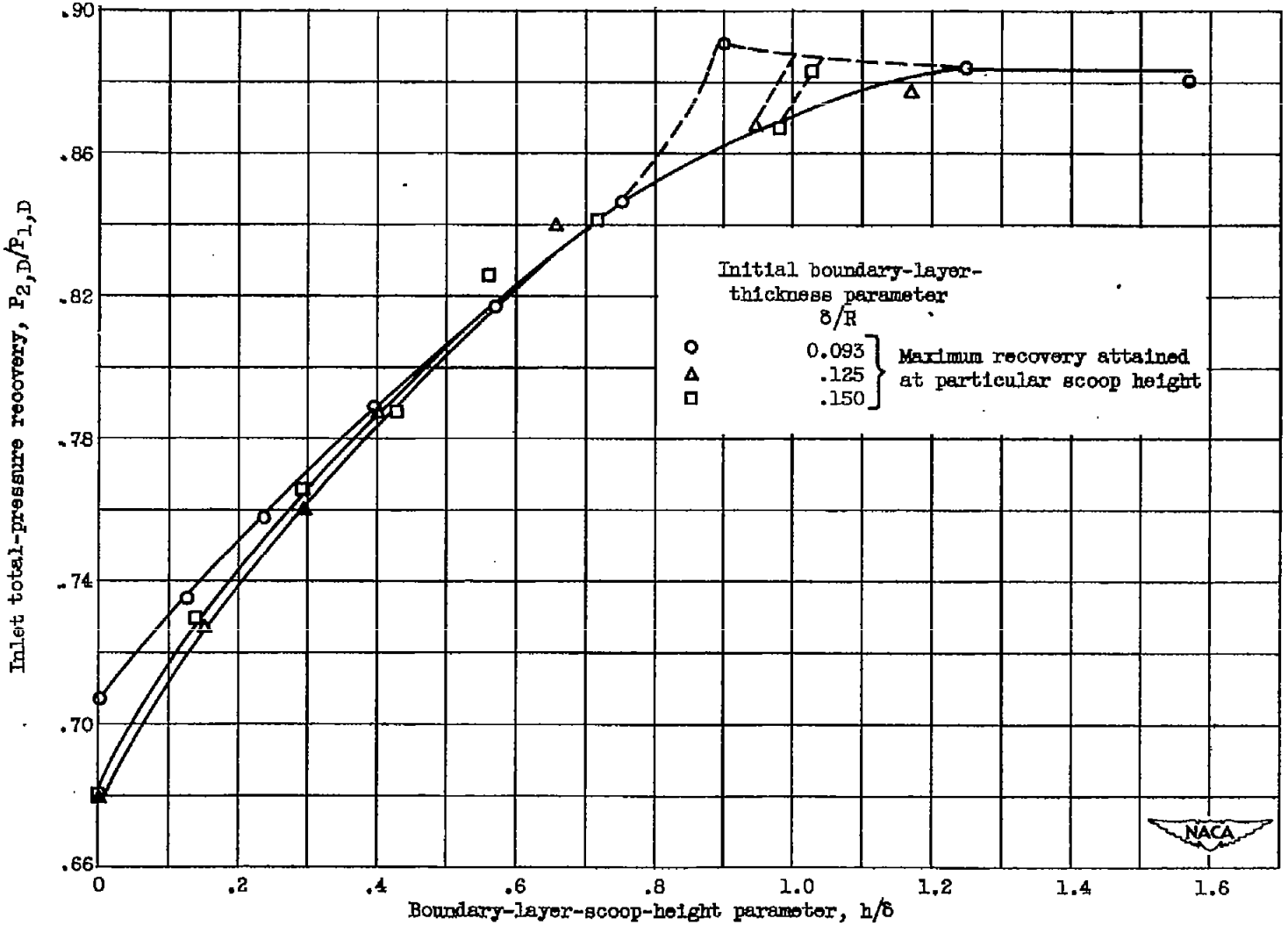

Figure 12. - Peak total-pressure recovery as a function of boundary-layer-scoop-height parameter for various initial boundary-layer thicknesses.

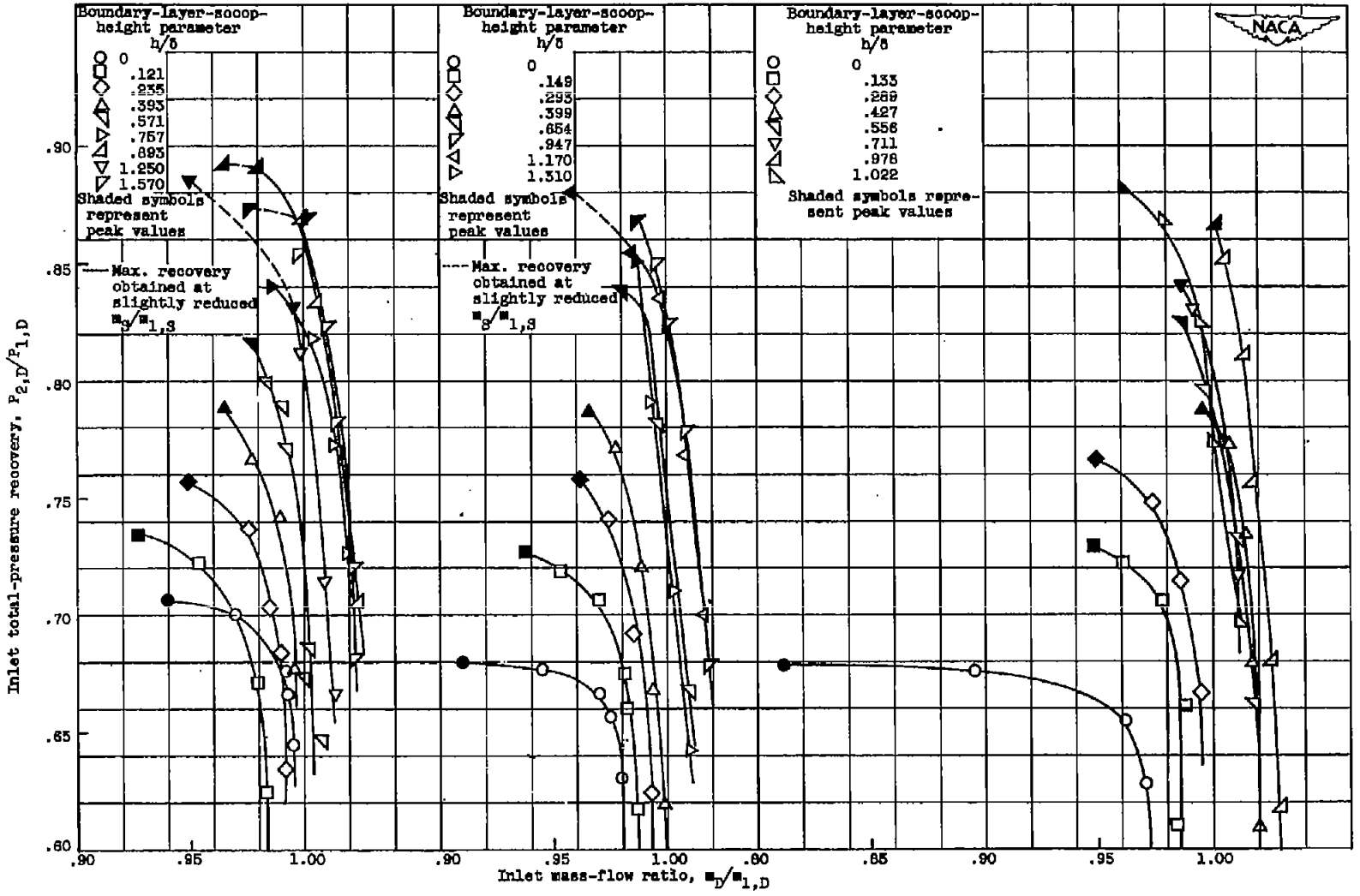

(a) Initial boundary-layer-thickness parameter δ/R, 0.095.

(b) Initial boundary-layer-thickness parameter δ/R, 0.125.

(c) Initial boundary-layer-thickness parameter δ/R, 0.150.

Figure 13. - Inlet pressure recovery as a function of inlet mass-flow ratio with supercritical boundary-layer-scoop operation.

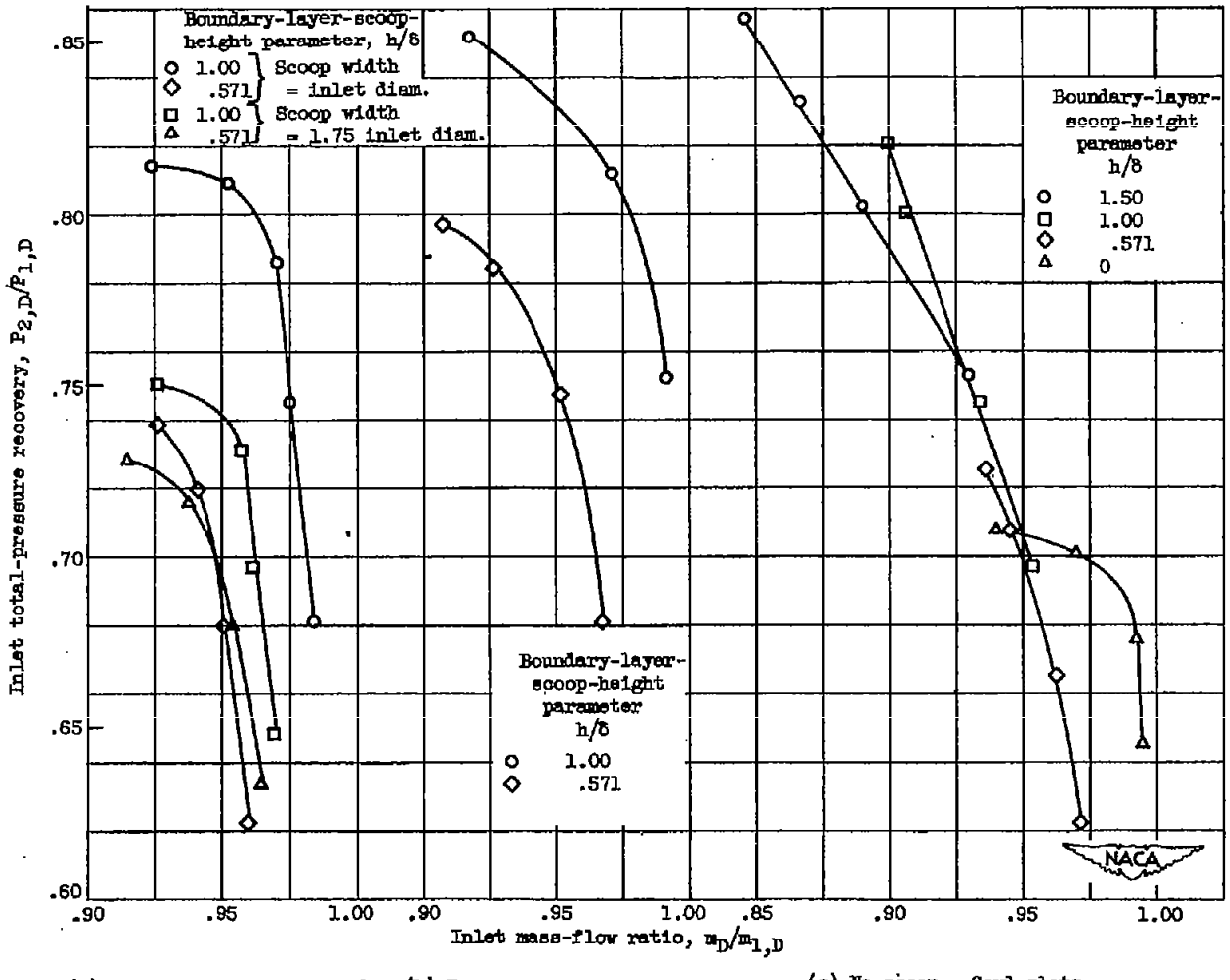

(a) Ram-type scoop with sides of duct removed and with straight leading edge.

(b) Ram-type scoop with sides of duct removed and with swept leading edge.

(c) No scoop. Cowl slots.

Figure 14. - Inlet pressure recovery as a function of inlet mass-flow ratio for alternative boundary-layer-removal systems with boundary-layer-thickness parameter of 0.085.

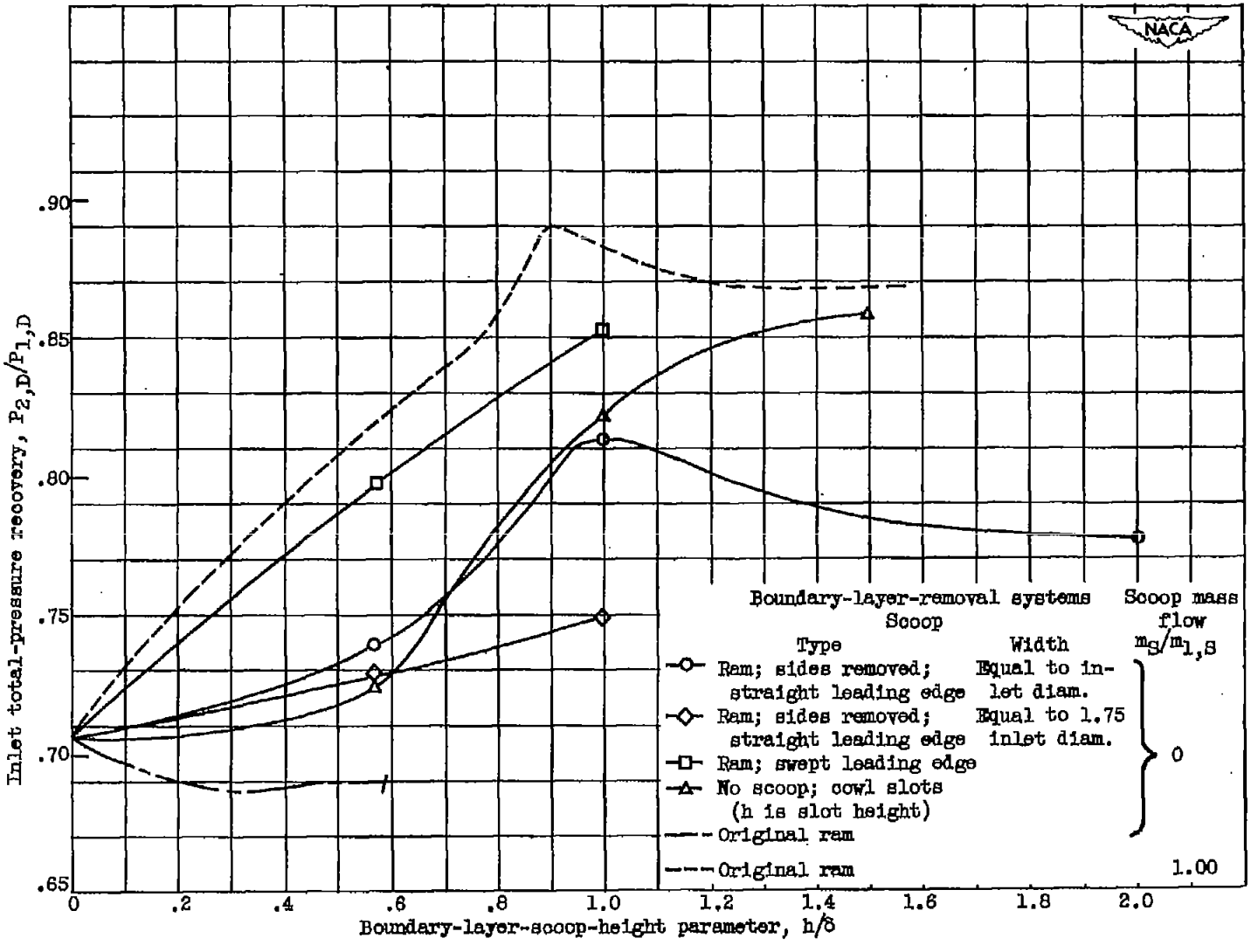

Figure 15. - Inlet peak total-pressure recovery as a function of boundary-layer-scoop-height parameter with various boundary-layer-removal systems and with an initial boundary-layer-thickness parameter of 0.093.

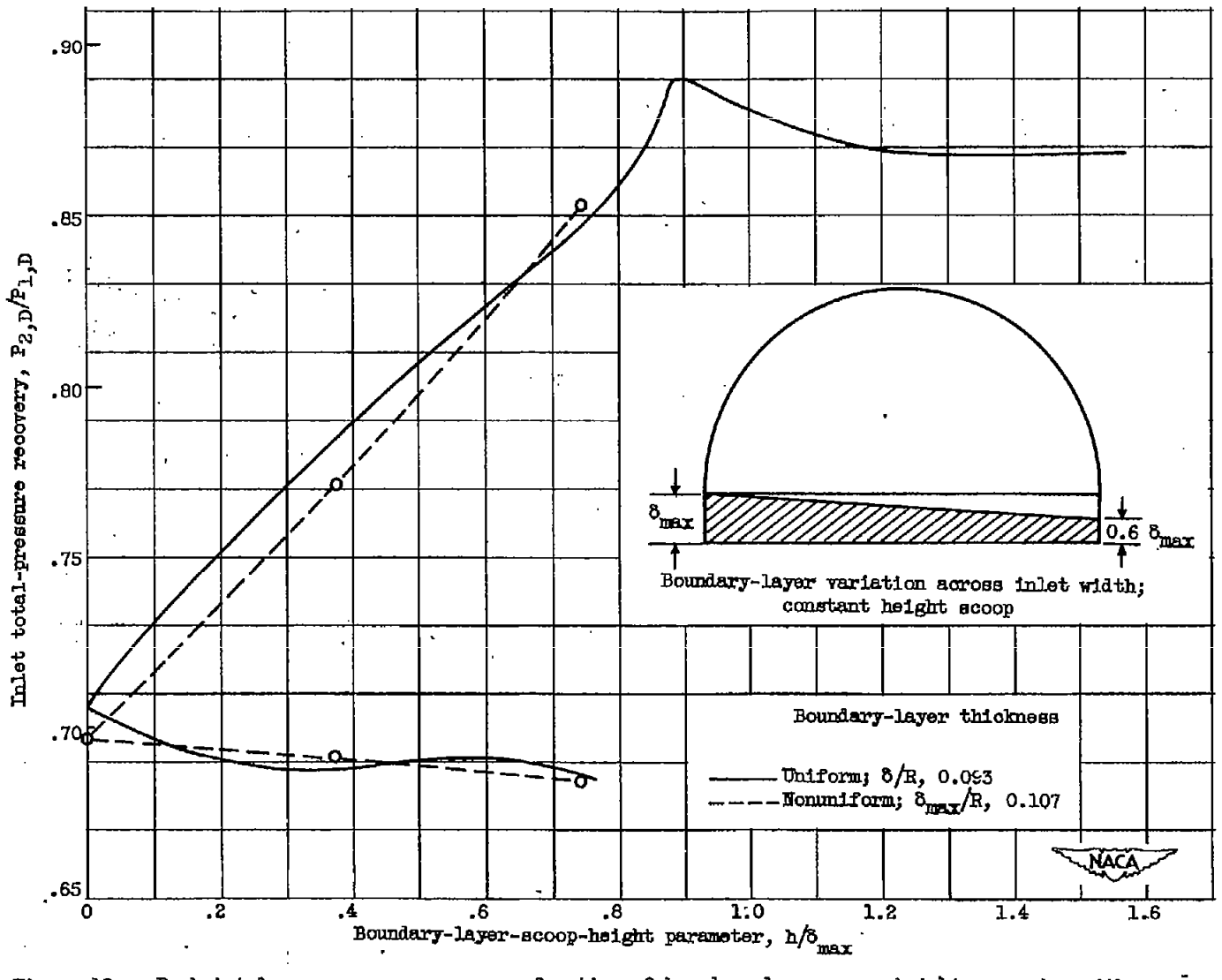

Figure 16. - Peak total-pressure recovery as a function of boundary-layer-scoop-height parameter with non-uniform boundary-layer thickness upstream of inlet.

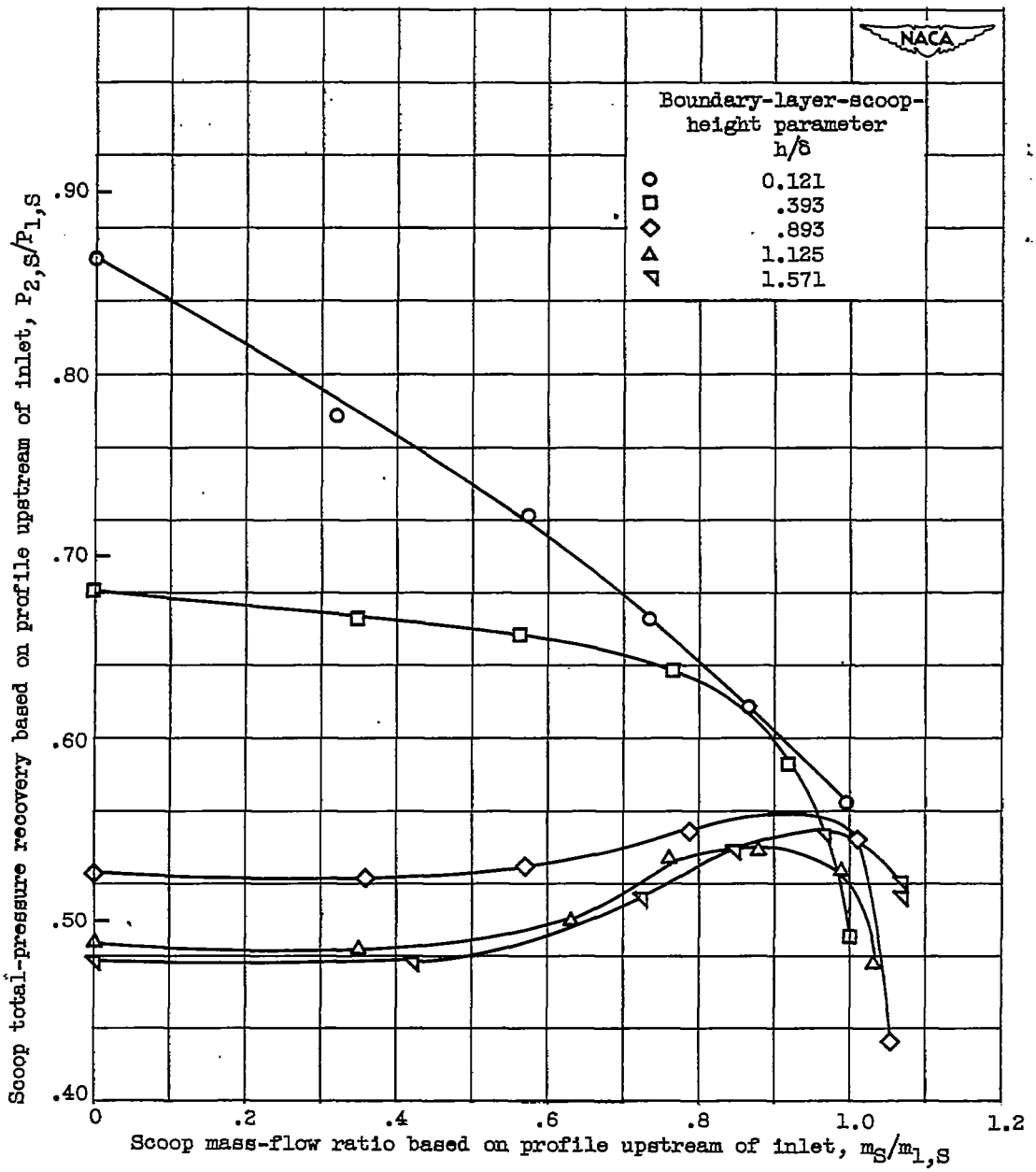

(a) Pressure recovery based on total-pressure profile upstream of inlet.

Figure 17. - Boundary-layer-scoop pressure recovery as a function of mass-flow ratio for various scoop heights and with initial boundary-layer-thickness parameter of 0.093.

[redacted]

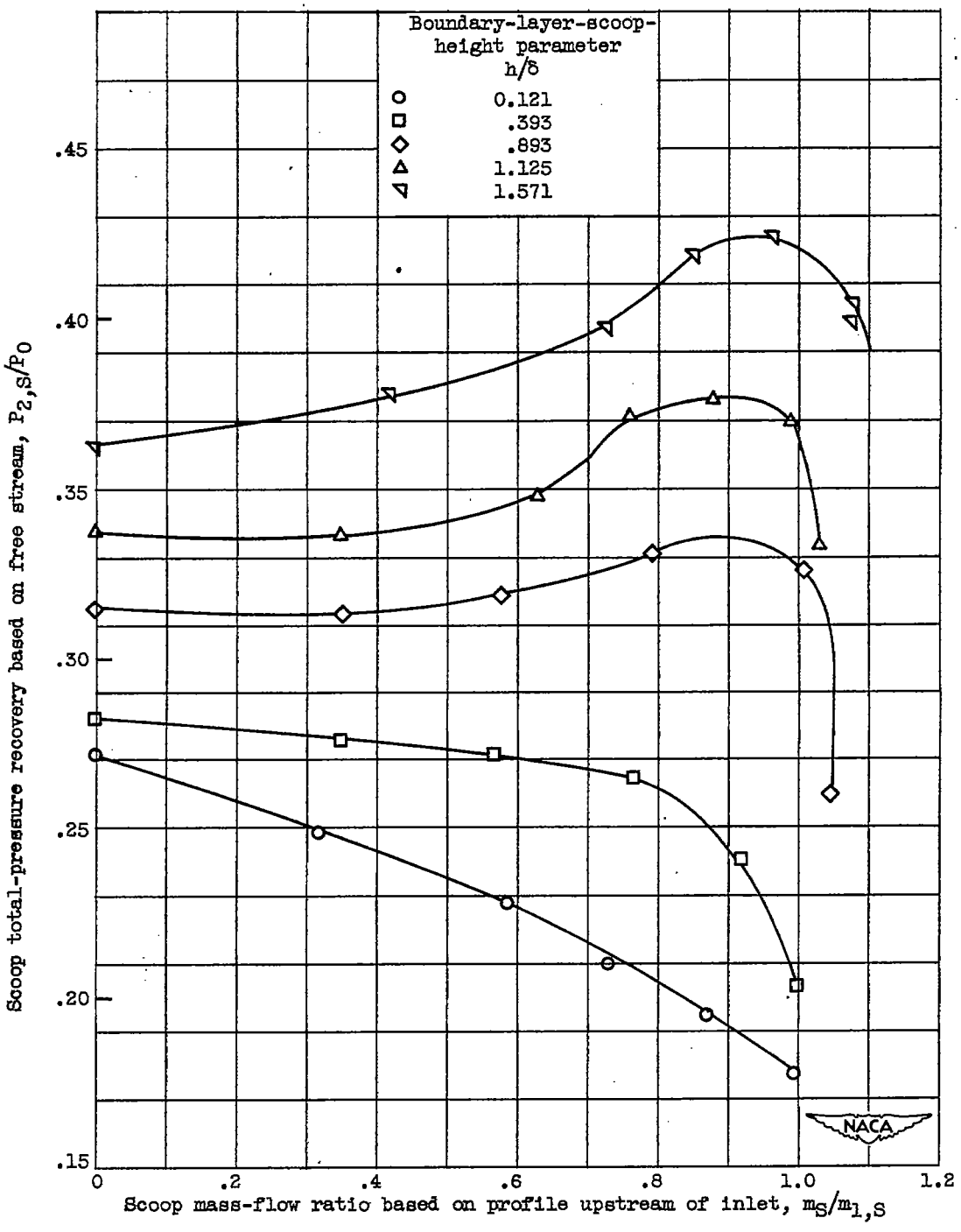

(b) Pressure recovery based on free-stream conditions.

Figure 17. - Concluded. Boundary-layer-scoop pressure recovery as a function of mass-flow ratio for various scoop heights and with initial boundary-layer-thickness parameter of 0.093.

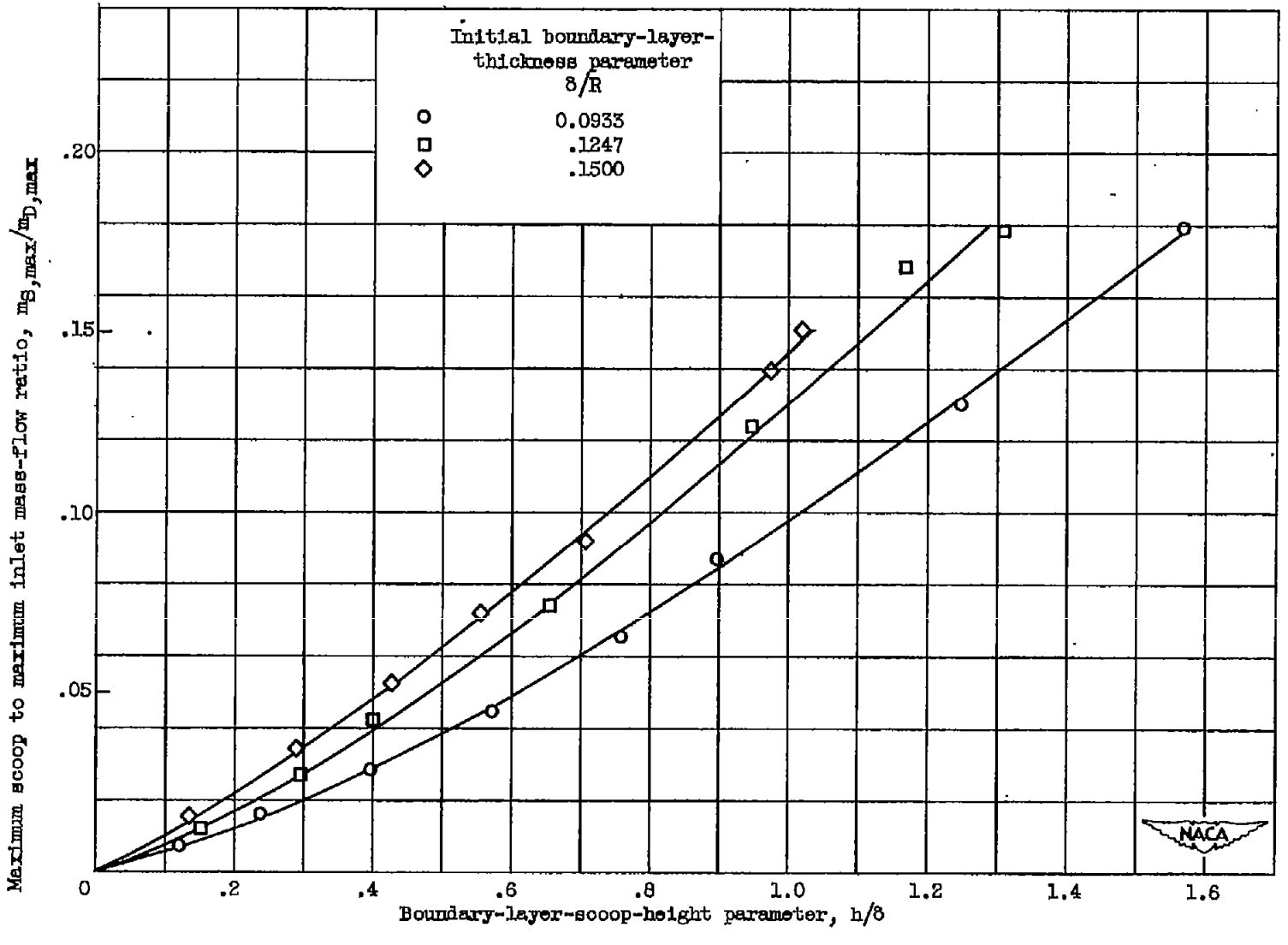

Figure 18. - Ratio of maximum scoop mass flow to maximum inlet mass flow as function of boundary-layer-scoop-height parameter.

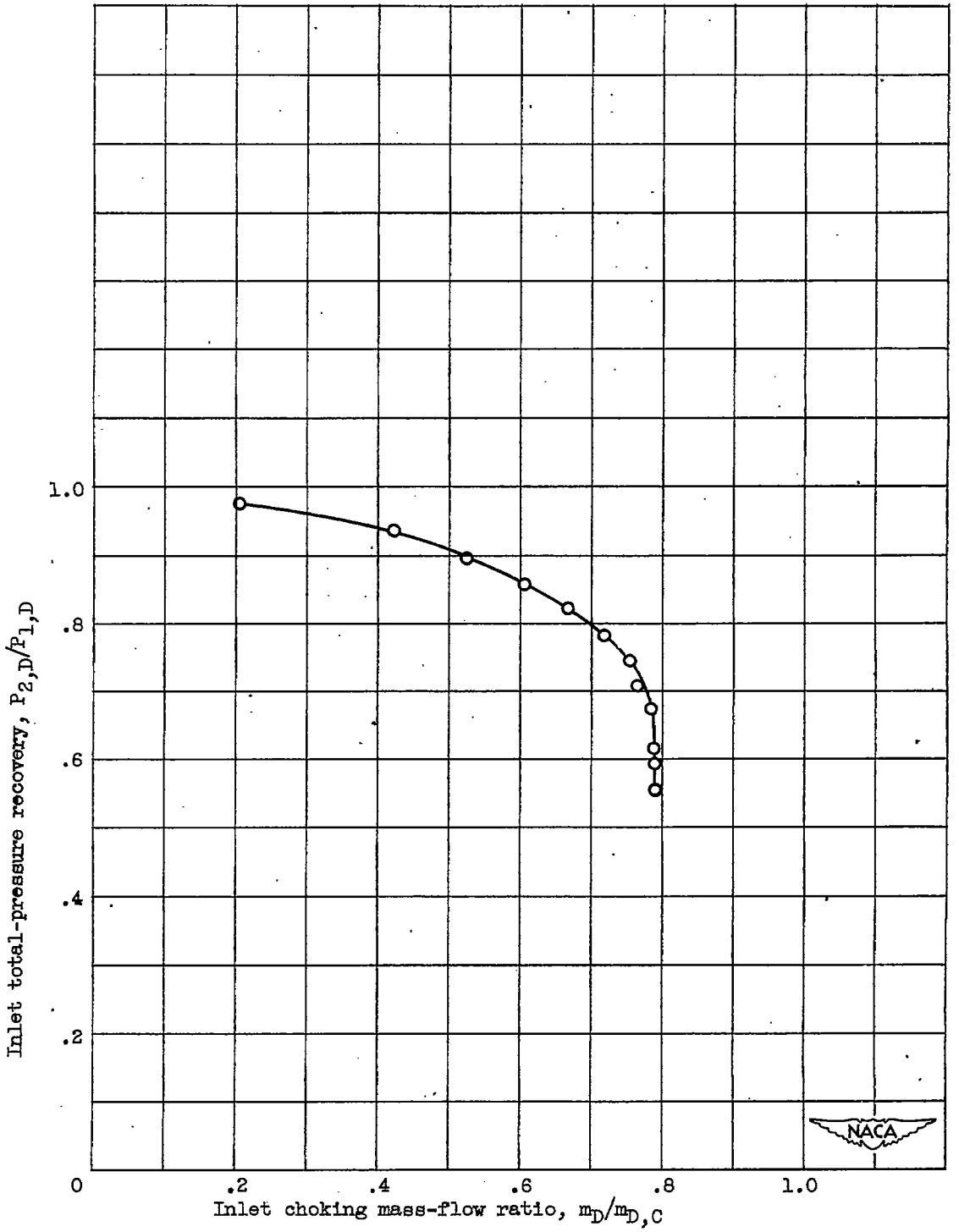

Figure 19. - Inlet pressure recovery at zero forward velocity as a function of inlet mass-flow ratio based on choking mass flow for the geometric throat.

NACA-Langley - 9-19-51 - 470